Transverse Jet Breakup and Atomization with Rapid Vaporization Along the Trajectory

J. A. Schetz,* P. W. Hewitt,† and M. Situ‡
Virginia Polytechnic Institute and State University, Blacksburg, Virginia

Experiments for transverse injection of chilled Freon-12 into the Virginia Tech 23×23 cm blowdown wind tunnel were run at a freestream Mach number of 0.44 and freestream stagnation pressure and termperature of 2.5 atm and 298 K, respectively. The spray plume was documented with photographs and droplet measurements. The results showed a clear picture of the mechanisms of jet decomposition in the presence of rapid vaporization. Immediately after injection, a vapor cloud was formed in the jet plume, which then dissipated downstream leaving droplets on the order of 8-10 μm in diameter. This represented a substantial reduction compared to base line tests run at the same conditions with water, which had little vaporization. A simulation approach to studying hot-flow, subsonic, cross-stream fuel injection problems in a less complex and costly cold-flow facility is proposed. The simulation parameters were developed and refined with the aid of a numerical solution for the simpler case of a rapidly evaporating laminar jet in a coaxial airstream. The experimental case was transformed through two new similarity parameters involving injection and freestream properties to a simulated case of a typical ramjet combustion chamber fuel injection problem where ambient temperature fuel (kerosene) is injected into a hot airstream.

Nomenclature

A = surface perturbation amplitude
D = mean droplet diameter
d = transverse distance
d_j = jet diameter
f = focal length of lens
h = penetration of plume
H = altitude
$I(\theta)$ = normalized intensity function
M = Mach number
p = pressure
Pr = Prandtl number
p_v = vapor pressure
$\bar{q}$ = jet/freestream momentum flux ratio $(\rho_j V_j^2/\rho_e V_e^2)$
Sc = Schmidt number
T = temperature
T^* = simulation parameter
T_B = boiling point
T_0 = stagnation temperature
V = velocity
$\bar{X}$ = x/d_j
x = downstream coordinate from injector
$\bar{Y}$ = y/d_j
y = vertical coordinate
θ = scattering angle
$\pi(T)$ = simulation parameter
ρ = density

Subscripts

j = jet conditions
e = main stream
pro = prototype conditions
sim = simulated conditions

Presented as Paper 83-0419 at the AIAA 21st Aerospace Sciences Meeting Reno, Nev., Jan. 10-13, 1983; received Jan. 29, 1983; revision received March 19, 1984.

*Professor and Department Head, Department of Aerospace and Ocean Engineering. Fellow AIAA.

†Graduate Student, Department of Aerospace and Ocean Engineering (presently with Atlantic Research Corp.). Member AIAA.

‡Visiting Scholar, Department of Aerospace and Ocean Engineering.

Introduction

FUEL jet injection plays a major role in the design of airbreathing engines such as ramjets or scramjets. Thus, extensive studies must be conducted into the effects of various injection parameters. This information is also valuable in the areas of thrust vector control, afterburners, liquid surface injection for cooling purposes, and external burning in the wake of projectiles. In the case of ramjet or scramjet engines, the fuel is usually injected from a wall or strut across an airflow.

Much work has been done on the mechanisms of jet decomposition, penetration of the liquid into the freestream, and atomization of the injectant (e.g., Refs 1-8). Comprehensive reports by Forde[2] and Schetz and Padhye[9] cover the effects of injection parameters and provide data correlations. Reichenbach[10] has studied the effects of injectant physical properties on jet structure, and Nejad and Schetz[11] have extended their studies to include droplet sizes in the plume. Virtually all of this work has been performed in a cold-flow situation, where an ambient temperature injectant is injected into ambient temperature air, and evaporation along the plume is not considered.

In order to take one step closer to the simulation of actual fuel injection in a hot-flow situation where ambient temperature fuel is injected into a heated airstream, this work will introduce the effects of evaporation and heating of the injectant along the plume by the airflow. The effect on droplet sizes, penetration, and jet structure will be investigated. This represents an advance in injection research even without consideration of droplet burning, since some combustor processes require the fuel sprays to be completely vaporized and mixed with air before reaction occurs in the combustion chamber. Therefore, fundamental data are required on droplet vaporization in heated gas streams.[12]

Detailed experimentation under the actual conditions to be encountered in a ramjet combustor is difficult and very expensive. To permit careful, laboratory environment studies covering a wide range of the important variables and parameters, a rational simulation procedure that allowed use of an unheated airstream would be valuable.

Experimental Methods

Test Matrix and Parameters

The most important similarity parameter associated with the fluid mechanics of transverse liquid injection is termed $\bar{q}$.

For this investigation, values of $\bar{q}=1$ and 4 were chosen for testing. A value of $\bar{q}=4$ is known as regime II injection,[2] which is a reasonable value for actual liquid fuel injection, and the test results may lend themselves to combustor problems. A value of $\bar{q}=1$ is classified as regime I[2], and the results may be directed more in the area of film cooling through surface injection.

In order to cover a range of the effects of evaporation, several chilled injection temperatures were studied for injection into a 298 K total temperature airstream. The Freon-12 was injected at temperatures ranging from 10 to -50°C.

Water was included in the test matrix to provide a simple base line case without significant evaporation for comparison. Those results are also of value in their own right, since rigorous studies of this type on droplet sizes in a subsonic water plume are limited.

The other airstream conditions were a total pressure of 2.5 atm and a Mach number of 0.44.

Spark Shadowgraphs

To observe the processes of injection and jet decomposition, short duration (10^{-8} s) spark shadowgraphs were taken to provide a stop-action look at the flowfield.

Streak Photographs

The purpose of this procedure was to obtain jet cross-stream penetration measurements at each condition as a function of distance downstream of the injector. Whereas a spark shadowgraph is a stop-action photograph, a streak photograph entails a longer exposure duration (10^{-3} s) that effectively integrates the unsteady jet motion over the exposure time. The penetration was measured directly from the photographs.

Droplet Size Distribution

The third type of testing undertaken was a determination of the mean droplet diameter at various locations in the jet plume. The method chosen to acquire this information was the diffractively scattered light method (DSLM). This method relates the pattern of scattered light to the mean droplet diameter in a small area of the jet plume. The details of the technique are discussed in Ref. 11. The method was used to determine a mean droplet diameter at $\bar{X}$ values of 10, 15, 25, 50, and 100 and $\bar{Y}$ values chosen according to penetration heights taken from the streak photographs.

Experimental Apparatus

Test Facility

The Virginia Tech 23×23 cm tunnel is a blowdown type with interchangeable test sections. For this work, a subsonic/transonic section was used. This has an adjustable downstream throat, facilitating the setting of the freestream Mach number. The Mach number was determined from static pressure taps mounted on the floor of the test section and the stagnation pressure measured upstream in the settling chamber. High-quality fused silica optical flats were used as windows.

Injection System

As previously mentioned, water and Freon-12 were chosen as the injectants. Some small differences in jet behavior, penetration, and droplet size may occur compared to actual hydrocarbon fuels due to small changes in surface tension and viscosity[11,13]; however, the results have been shown to be similar enough to extend the data obtained to combustor problems.

The water was delivered from a storage tank pressurized with nitrogen, and the mass flow rate was measured with a calibrated Rotameter.

A more complex arrangement was necessary to deliver the Freon-12 due to the need for careful attention to the injection temperature. The Freon-12 was stored in commercial disposable tanks. It first passed through a specially built heat exchanger tank. The heat exchanger consisted of a cast iron vessel surrounded by Styrofoam insulation containing a bath of ethyl alcohol with an immersed coil of copper tubing through which the Freon-12 was passed. Dry ice was added to the ethyl alcohol until the desired coolant temperature was reached. The cooled Freon-12 was then passed through a cryogenic flow meter. Two bellows-type cryogenic valves were used to adjust the flow rate.

The Freon-12 and water were injected into the wind tunnel through a removable injector assembly. The assembly consisted of an insulated central duct leading to a 0.91 mm diam orifice. A thermocouple was placed directly in the injectant flow to monitor the injectant temperature. The injector was fitted flush with the floor of the wind tunnel so as not to create any disturbance in the flowfield. A sketch is shown in Fig. 1.

Optical Equipment

To obtain spark shadowgraphs, a Nanopulser flash was used to backlight the plume. A 20 cm focal length lens was used to focus the image on a Polaroid film carrier. Type 57 Polaroid film was used ((ASA 3000) because a high sensitivity was required due to the extremely short exposure time.

A mercury arc lamp was used with a parabolic mirror to deliver an intense parallel light source for the streak pictures. This light was used to backlight the plume in the test section. Type 55 Polaroid film (ASA 50) was used, since a high sensitivity was not required.

Diffractively Scattered Light Method Apparatus

The method chosen to determine the droplet diameters in the plume was the DSLM, which relates light scattering to droplet diameters in a spray. For a detailed description of the theory behind this method, see Refs 11 and 14-17. The information required for this method is light intensity as a function of scattering angle. The intensities are then normalized with the unscattered light intensity in the forward direction ($\theta=0$), forming a normalized scattering function $I(\theta)$. Once these values are obtained, the mean droplet diameter can be obtained from the theoretical illumination profile as compiled by Gooderum and Bushnell.[15]

A 15 mW helium neon laser was chosen as the light source. The beam was further filtered with a spatial filter that delivered a thin, parallel beam of intense light. The laser beam passed through the wind tunnel test section, penetrating the jet plume. The two windows and the laser beam had to be perfectly aligned to eliminate interference patterns. A photomultiplier enclosed in a tube and mounted on a traverse was used to measure the light intensity.

The scattered light was collected with a 50 cm focal length lens. Since the plume is located at the focal length of the lens,

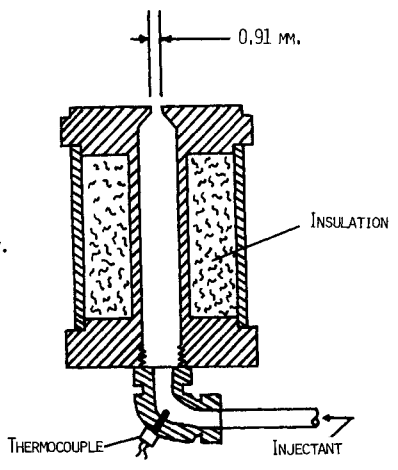

Fig. 1 Injector assembly.

the scattered light is parallel when it emerges from the lens, and the scattering angle can be related to the traverse position from the relation $\theta = \tan^{-1}(d/f)$. This arrangement worked well for droplet sizes down to about 15 μm; however, to measure smaller droplets, it was necessary to scan at greater angles. For this reason, a different optical arrangement was devised as shown in Fig. 2. In this scheme, the collecting lens could be placed closer than the focal length and, upon applying basic lens laws, the scattering angle can be found as a function of the traverse distance d. Since the voltages obtained from the photomultiplier varied greatly, a logarithmic amplifier was used to process the signal.

Experimental Results

Jet Plume Structure

Spark shadowgraphs of water injected at $\bar{q} = 1$ and 4 are shown in Fig. 3. The processes of jet decomposition are evident, involving the formation of short high-amplitude waves and the breakup into clumps and then droplets. These processes follow the same general patterns as breakup in a supersonic crossflow (see Ref. 2).

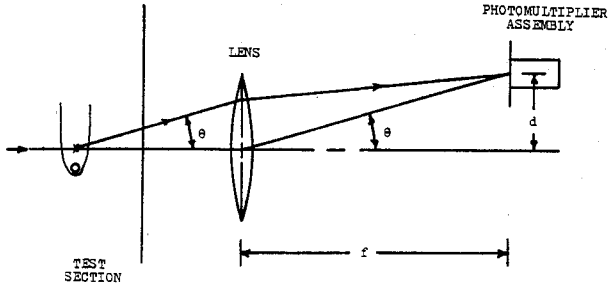

Fig. 2 Optical arrangements for droplet size measurements.

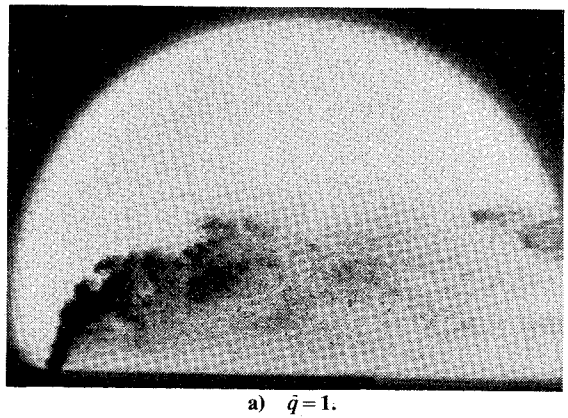

a) $\bar{q} = 1$.

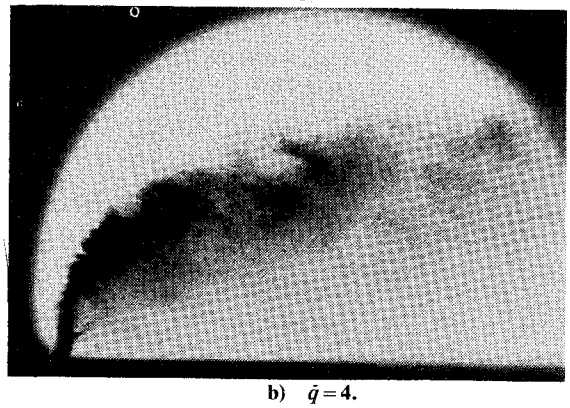

b) $\bar{q} = 4$.

Fig. 3 Spark photographs of water injection (negligible vaporization).

It is the main intent of this work to examine a case where evaporation of the injectant plays an important part in the atomization mechanisms. The first sequence of photographs are spark shadowgraphs of Freon-12 injected at $\bar{q} = 4$ (Fig. 4). The photographs are arranged in order of increasing injectant temperature. The first observation to be made is the cloud-like appearance of the plume. This is unlike the water case

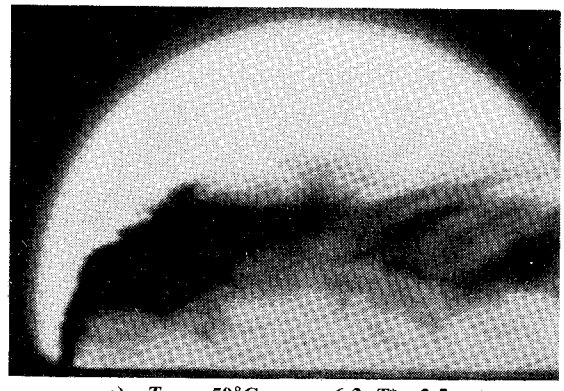

a) $T_j = -50°\text{C}$, $\pi_j = -6.3$, $T^* = 2.5$.

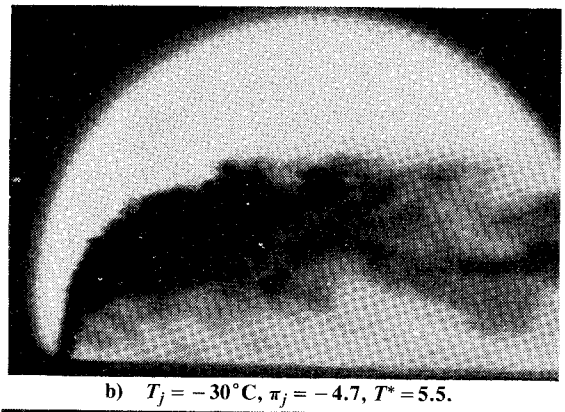

b) $T_j = -30°\text{C}$, $\pi_j = -4.7$, $T^* = 5.5$.

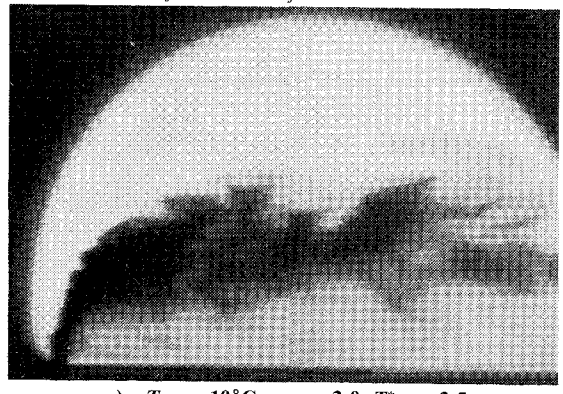

c) $T_j = -10°\text{C}$, $\pi_j = -3.0$, $T^* = -3.5$.

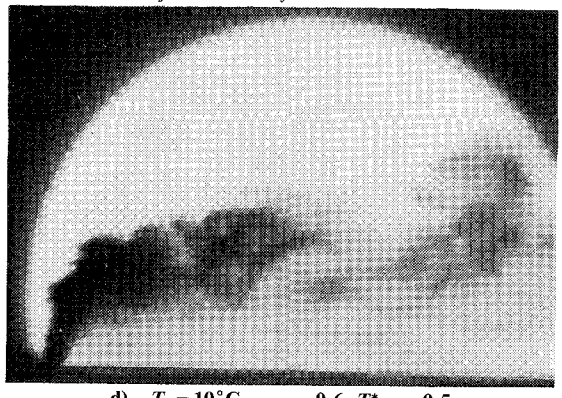

d) $T_j = 10°\text{C}$, $\pi_j = -0.6$, $T^* = -0.5$.

Fig. 4 Spark shadowgraphs of Freon-12 injection at $\bar{q} = 4$.

where the distinct formation of individual droplets is clearly seen. It is possible, however, to view larger droplets in areas where the cloud is less dense. For this reason it would seem that the process of initial jet decomposition is not an immediate "flashing" of the injectant, but a wave mechanism similar to that of water. The subsequent heating and evaporation of the injectant along the plume accounts for the fog-like appearance of the jet plume. As the temperature of the injectant is increased, it is seen that the fog is "burned off" at a more rapid rate.

The second sequence of photographs shows spark shadowgraphs of Freon-12 injected at a $\bar{q}=1$ (Fig. 5). In these photographs, since the $\bar{q}$ value has decreased from 4 to 1, the Freon-12 is injected at a lower velocity. The same observations can be made for these flows concerning the mechanisms of jet decomposition. The primary difference for the case of a lower value of $\bar{q}$ is that, due to a decreased jet injection velocity, the fluid penetrates less into the freestream, and the plume closely follows the model surface.

Penetration

The datum obtained from the streak photographs is the penetration of the jet plume into the freestream. For each case in the test matrix, a streak photograph was taken and the data were used to determine a judicious placement of droplet diameter sampling. Additionally, the penetration was measured at a location of 20 diameters downstream of the injector for each test case. These results are plotted as nondimensional penetration (h/d_j) vs $\bar{q}^{1/2}$ in Fig. 6. As can be seen, there is a small reduction in penetration over the range of conditions compared to nonevaporating water injection. A slightly higher penetration is noted for the case of Freon-12 at 10°C. This was likely due to intermittent cavitation in the delivery lines causing bursts of fluid to be injected at a greater velocity than intended for this case.

Droplet Size Distribution

The optical arrangement utilized for the DSLM yielded an average droplet diameter in an area the size of the laser beam (0.071 cm^2). The results of these measurements are shown in Fig. 7 for the case of water at $\bar{q}=1$ and 4. The $\bar{X}$ and y/h axes locate the space coordinates along the plume, and mean droplet diameters are plotted along the normal axis. These results show that, for injection at $\bar{q}=4$, the larger droplets initially occupy a region close to the upper edge of the plume. As they are carried downstream, they become more evenly distributed along the plume centerline and then gradually settle closer to the injection plane. It should also be noted that the droplet diameters are decreasing in the downstream direction as further atomization and evaporation take place.

The results for water injected at $\bar{q}=1$ show a slightly different droplet distribution. At all stations considered, the larger droplets remained in the lower portion of the jet plume. Again, as the droplets travel downstream, the mean droplet diameters decrease. It can also be observed that at virtually all stations the droplets are larger for the lower injection rate.

The results for water can be generalized as follows: 1) by increasing $\bar{q}$, smaller droplets result; 2) as the downstream distance from the injector increases, the mean droplet diameter decreases; and 3) the larger droplets eventually migrate to the lower portion of the plume for the case of a higher dynamic pressure ratio, whereas for a lower $\bar{q}$, the larger droplets are always found close to the wall.

These results for water injection can be combined with the photographs of the jet plume to convey a complete picture of how the jet plume behaves for cases with negligible evaporation.

As was previously mentioned with the spark shadowgraphs, a cloud of very small droplets surrounds the jet plume when the readily evaporated Freon-12 is injected. Because the

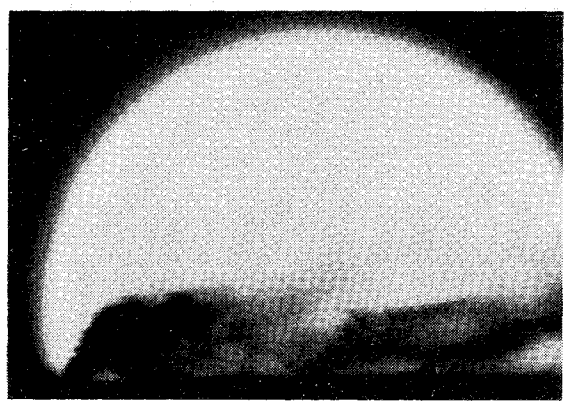

a) $T_j=-50°C$, $\pi_j=-6.3$, $T^*=2.5$.

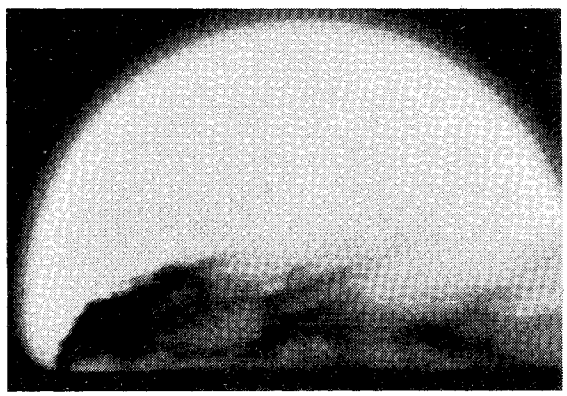

b) $T_j=-30°C$, $\pi_j=-4.7$, $T^*=5.5$.

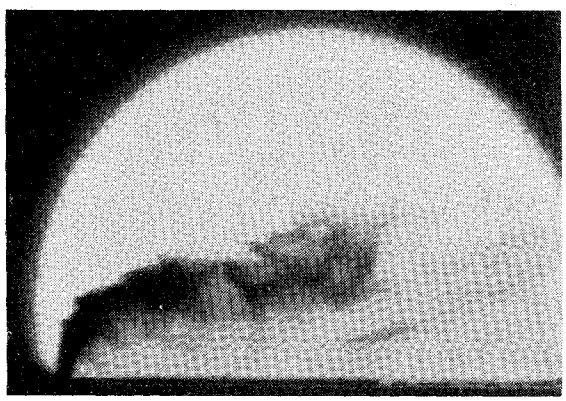

c) $T_j=-10°C$, $\pi_j=-3.0$, $T^*=-3.5$.

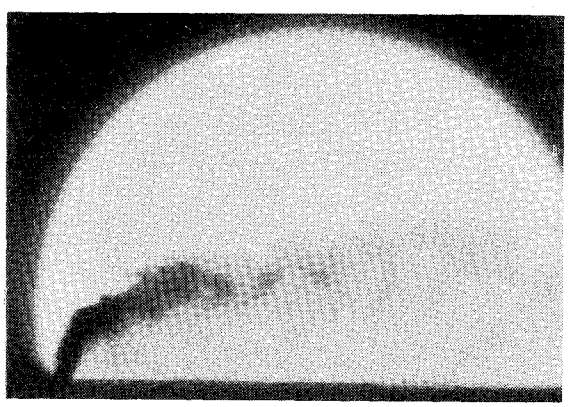

d) $T_j=10°C$, $\pi_j=-0.6$, $T^*=-0.5$.

Fig. 5 Spark shadowgraphs of Freon-12 injection at $\bar{q}=1$.

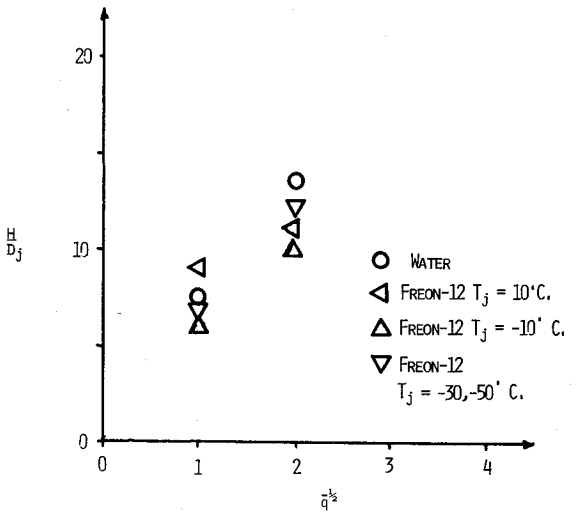

Fig. 6 Cross-flow penetration results.

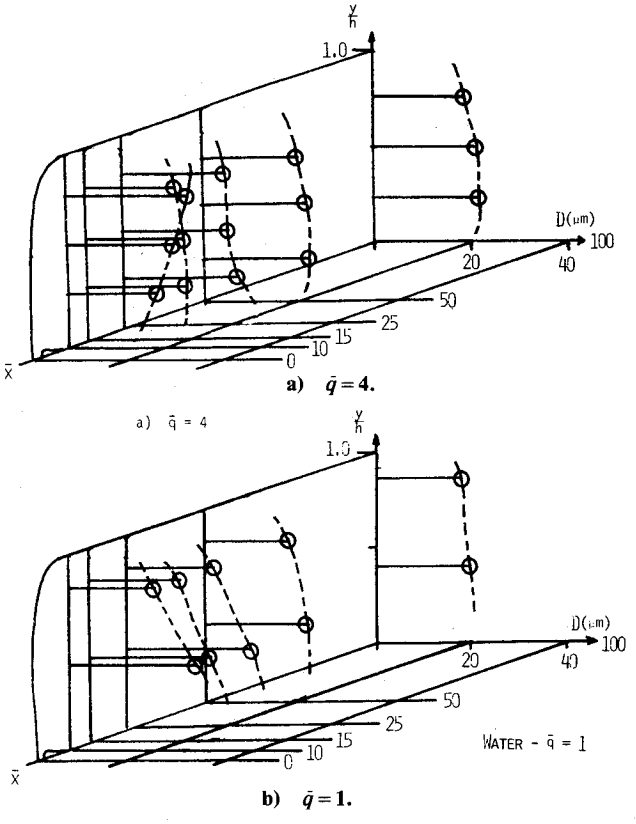

a) $\bar{q}=4$.

b) $\bar{q}=1$.

Fig. 7 Droplet size distributions in the plume for water injection (negligible vaporization).

DSLM is based on the scattering of light, the cloud presents problems because of increased absorption of the laser beam and multiple scattering, since the number of droplets is increased greatly. These factors made the DSLM inappropriate for determining droplet sizes in the early sections of the plume for these test conditions. Droplets can be seen in the spark shadowgraphs, but the majority are obscured by the vapor cloud, making droplet measurements directly from the photographs difficult. It was found, however, that measurements with the DSLM could be used farther downstream after some of the cloud had evaporated. The thinning effect of the vapor cloud was noted by Reichenbach,[10] where it was observed that a plume of a highly evaporating injectant became less dense after a location of $x/d_j > 50$. For these reasons, measurements were made here at a location of $x/d_j = 100$.

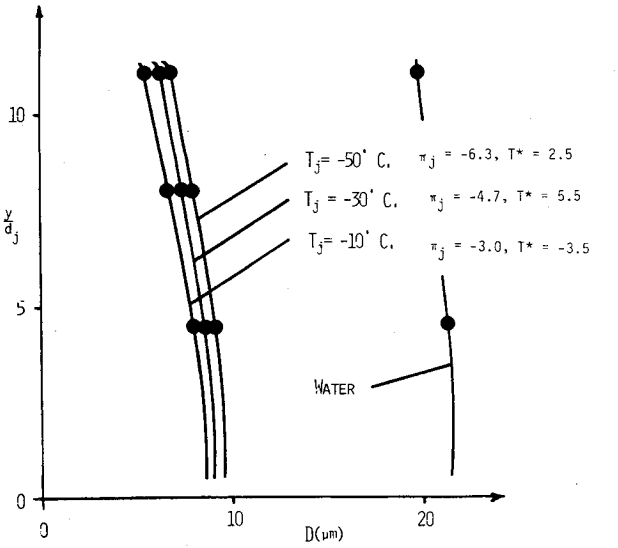

Fig. 8 Droplet size variation for Freon-12 injection at $\bar{X}=100$ with $\bar{q}=4$.

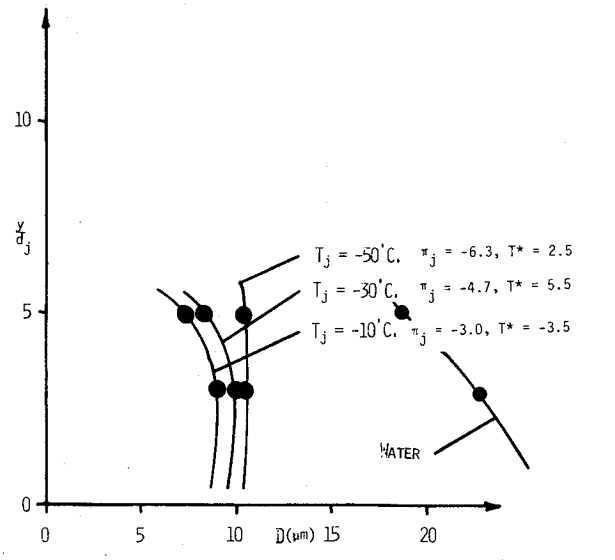

Fig. 9 Droplet size variation for Freon-12 injection at $\bar{X}=100$ with $\bar{q}=1$.

The results for Freon-12 injected at $\bar{q}=4$ and $T_j = -10$, -30, and $-50°C$ are shown in Fig. 8, and the results for $\bar{q}=1$ are shown in Fig. 9. Data for $T_j = 10°C$ were not included due to intermittent cavitation in the delivery lines causing inconsistent readings.

Upon examining the data for the case with $T_j = -50°C$ and $\bar{q}=4$, it can be seen that the profile of the droplet sizes is similar to water injection with the larger droplets lower in the plume. However, the droplet diameters have been reduced an average of 55% from the water case. By raising the injection temperature to $-30°C$, the rate of evaporation is increased. The average droplet diameter at this station drops 10%. By increasing the injection temperature even further to $-10°C$, the average droplet size is decreased an additional 6%.

Derivation of a Simulation Scheme

If we could derive a suitable simulation scheme, the results of studies such as those discussed above could be directly applied to real, hot-flow cases. The derivation of a rigorous scheme of that type is obviously difficult, but we present the following heuristic development as a first step toward that goal.

The simulation problem that we wish to address can be stated as follows: if all the mechanical aspects of the prototype and model injection problems are matched except heating, how can the effects of heating and thus vaporization along the plume be simulated with an ambient temperature airflow? Thus, we will require at least close matches of injector size and shape, injectant flow rate (expressed as $\bar{q} \equiv \rho_j V_j^2 / \rho_e V_e^2$), cross-flow Mach number and injectant density, viscosity, and surface tension. This would be enough to insure equivalence if heating were not important. In the prototype case, ambient temperature fuel is injected across a hot-airstream. At the injection temperature, the vapor pressure is low and there is little evaporation. As the liquid is heated along the trajectory of the jet, the vapor pressure rises rapidly and there is substantial evaporation. Therefore, there is some time history of temperature (and vapor pressure) along the plume, and that is the process we wish to simulate. Here, as with all problems involving heat and mass transfer, one can also anticipate that the Prandtl and Schmidt numbers will be important.

To put this all on a rational basis, we introduce nondimensional expressions involving the vapor pressure and the driving force for heating—the difference between the injection temperature and the air stagnation temperature. The relevant reference point for the local vapor pressure is the static pressure. This difference can be normalized with the dynamic pressure, so we choose the parameter

$$\pi(T) \equiv \frac{p_v(T) - p_e}{\frac{1}{2}\rho_e V_e^2} \tag{1}$$

This can be recognized as what is often termed a cavitation number in a quite different context.

For a dimensionless temperature difference, we can write

$$T^* \equiv \frac{T_{0,e} - T_j}{T_{\text{ref}}} \tag{2}$$

where T_{ref} is some suitable characteristic temperature or temperature difference. A simple choice for T_{ref} might be just $T_{0,e}$, but that has no foundation in physical reasoning. It would seem that the boiling temperature of the injectant T_B should provide a suitable reference point. However, it is obviously difficult to make a proper selection based on physical reasoning alone. Thus, we have adopted the use of an essentially exact numerical solution procedure for a much simpler, but related, problem to aid in the selection process for T_{ref} and to test the whole scheme.

The computer code developed in Ref. 18 treats the axisymmetirc Navier-Stokes equations for an evaporating, laminar liquid jet in a low-speed, coflowing stream. That problem can be viewed as an idealized version of the problem of interest here. Thus, a suitable simulation scheme should certainly apply to this idealized problem, and we can use the computer code to run "numerical" experiments to see if a trial simulation provides a true cold-flow simulant to a hot-flow case.

To illustrate the process and the results, consider as case I a prototype ramjet engine traveling at a freestream Mach number of 2.34 at 18,300 m. Assuming diffusion to a Mach number of 0.44 in the combustor yields a stagnation temperature of 453 K in the combustor entrance plane and a stagnation pressure of 0.972 atm. Now consider kerosene fuel injected at 20°C. At this point $p_v = 0.05$ atm, so $(\pi)_{\text{pro},j} = -6.75$. The task is now to transform the process into one that can be implemented in a cold-flow wind tunnel facility. The wind tunnel freestream Mach number can be taken as that in the combustor for the real case, $M_c = 0.44$. In establishing a value for the stagnation pressure, a compromise must be reached between operable values for the wind tunnel available and the satisfaction of matching requirements. A value of 1.14 atm adequately satisfied these needs, generating the pressure ratios. This value fixes the freestream static and dynamic pressure at 1.0 and 0.138 atm, respectively. The stagnation temperature of the facility was taken as that of ambient air. With these figures, a fluid must be found such that the values of π and T^* are matched with the real case at injection and at the tunnel stagnation conditions. Of course, we have not yet fully defined T^*. Skipping all the details of our trial-and-error efforts at selecting T_{ref}, we can summarize the results by saying that $T_{0,e}$ will not serve and that the choice $T_{\text{ref}} \equiv (T_B - T_j)$ proved suitable. For our case I, this gives $(T^*)_{\text{pro},j} = 1.35$. At injection, the value of $(T^*)_{\text{sim},j}$ must be 1.35. Since the wind tunnel stagnation temperature is known, this fixed the injection temperature at -50°C. Therefore, a model fluid had to be found with a vapor pressure of 0.051 atm at -50°C in order to match the conditions at injection, $(\pi)_{\text{sim},j} = -6.75$. Freon-21 is found to have a vapor pressure of 0.0505 atm at -50°C. The physical property values and density are also a reasonable match with kerosene. The similarity parameters are summarized in Table 1.

Now, we can use the numerical method to calculate idealized versions of the prototype (hot-flow) and simulated (cold-flow) cases in order to study the time history of two different liquid jets in airflows at the different stagnation temperatures. If the time history of the two liquid jets is equivalent, we can say that the cold-flow case is a good simulant of the prototype (hot-flow) case. Figure 10 shows the numerical results for case I. The plot gives the time variation of the "crests" and "troughs" on the liquid jet column that grow and lead to breakoff and drop formation. Note that the troughs grow faster than the crests. If the simulation scheme proposed here were perfect, the results for the prototype and simulated conditions would be identical. Figure 10 shows that good simulation of the hot case has been achieved, with the results for the important troughs (that lead to breakoff) being excellent.

Encouraged by the favorable results obtained above, we were emboldened to try another case. Consider for case II, a prototype ramjet with heated fuel (e.g., by regenerative cooling) and now traveling at a freestream Mach number of 2.81 at 18,300 m. Assume again that diffusion to a Mach number of 0.44 in the combustor yields a stagnation temperature of 558 K and a stagnation pressure of 2.01 atm. Now consider kerosene fuel injected at 40°C. At this point $p_v = 0.11$ atm so, $(\pi)_{\text{pro},j} = -6.35$, and $(T^*)_{\text{pro},j} = 2.5$. The wind tunnel freestream Mach number is taken the same as

Table 1 Parameters for case I

Parameters	Kerosene hot prototype case	Freon-21 cold simulated case
M_∞	2.34	Wind tunnel
H, m	18,300	—
T_0, K	453	300
M_c	0.44	0.44
T_j, °C	20	−50
T_B, °C	138	9
T_0, °C	180	27
π_j	−6.75	−6.9
T_j^*	1.35	1.35
Viscosity at T_j, N·S/m^2	1.49×10^{-3}	0.72×10^{-3}
Density at T_j, kg/m^3	0.82×10^3	1.37×10^3
Surface tension at T_j, N/m	27.2×10^{-3}	33.8×10^{-3}
Heat of vaporization, J/kg	2.42×10^5	2.40×10^5

Table 2 Parameters for case II

Parameters	Kerosene hot prototype case	Freon-12 cold simulated case
M	2.81	Wind tunnel
H, m	18,300	—
T_0, K	558	298
M_c	0.44	0.44
T_j, °C	40	−50
T_B, °C	138	−20
T_0, °C	285	25
π_j	−6.35	−6.3
T_j^*	2.5	2.5
Viscosity at T_j, N·S/m^2	1.1×10^{-3}	0.76×10^{-3}
Density at T_j, kg/m^3	0.78×10^{-3}	1.3×10^{3}
Surface tension at T_j, N/m	26.3×10^{-3}	31.5×10^{-3}
Heat of vaporization, J/kg	2.42×10^{5}	1.68×10^{5}

Table 3 Range of injection parameters for experiments with Freon-12

T_j, °C	p_v, atm	π_j	T_j^*
−50	0.39	−6.30	2.5
−30	0.83	−4.72	5.5
−10	1.32	−3.03	−3.5
10	2.02	−0.62	−0.5

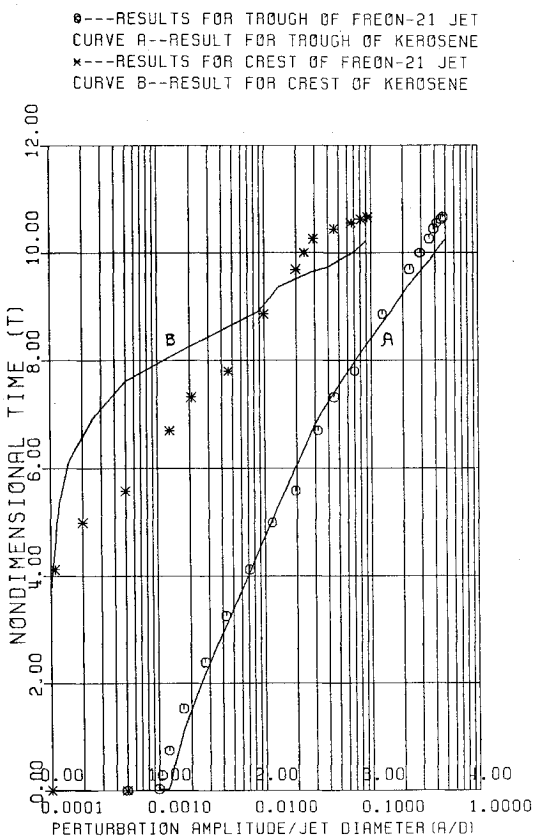

Fig. 10 Calculated growth of surface disturbances vs time for kerosene and Freon-21 jets, simulation test case I.

that in the combustor for the real case, $M_c = 0.44$. A value of 2.5 atm for the total pressure adequately satisfied these needs. This fixes the freestream static and dynamic pressure at 2.20 and 0.29 atm, respectively. The stagnation temperature of the facility was again ambient. With these figures, a fluid must be found such that the values of π and T^* are matched with the real case at injection and at tunnel stagnation conditions. Therefore, a model fluid had to be found with vapor pressure of 0.39 atm at −50°C in order to match the conditions at injection $\pi_{\text{sim},j} = -6.35$. Freon-12 is found to have a vapor pressure of 0.388 atm at −50°C. The physical property values and density are also a reasonable match for kerosene. The similarity parameters are summarized in Table 2.

Figure 11 shows the numerical results for case II. As can be seen, the time history of the liquid jet in the prototype case is closely simulated by the cold-flow case. The poorest correspondence is at the very beginning of the time history, because the vaporization of the Freon-12 jet is faster.

Most importantly, we can tentatively conclude from this comparison between the numerical predictions for the prototype and simulated conditions for two cases that the simulation method proposed is capable of simulation of hot prototype cases in cold wind tunnel tests. In the language of mathematics, we have apparently demonstrated "sufficient" conditions for simulation, but we have not demonstrated whether these conditions are also "necessary." However, the general problem is very complex and a workable "sufficient" simulation scheme is very useful.

Application of the Derived Simulation Scheme

The experimental conditions studied can be restated in terms of our two simulation parameters, π and T^*, as in Table 3. Looking at Table 2, it can be seen that the experimental case with $T_j = -50$°C ($\pi_j = -6.30$ and $T_j^* = 2.5$) matches the simulated case II. Thus, the results for our $T_j = -50$°C, $\bar{q} = 4$ experiments (see Figs. 4a, 6, and 8) provide results that can be

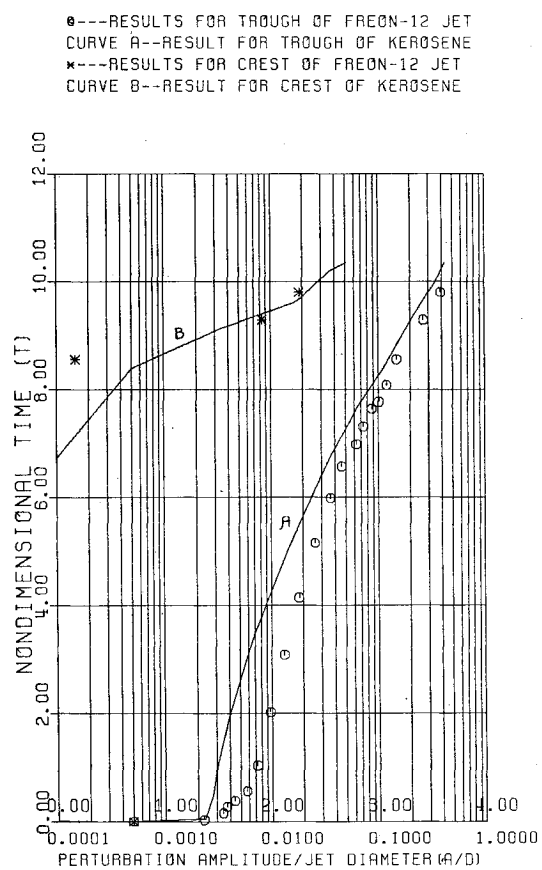

Fig. 11 Calculated growth of surface disturbances vs time for kerosene and Freon-12 jets, simulation test case II.

applied to the hot prototype conditions of case II ($M_\infty = 2.81$, $H = 18{,}300$ m, $M_c = 0.44$, $T_j = 40°C$). In particular, by comparing with our results for water injection (negligible evaporation), one can conclude that the droplet sizes would be reduced by about 55% in the hot-flow case compared to predictions neglecting vaporization.

Conclusions

The introduction of evaporation and heating considerations over a baseline case of water injection can result in a decrease in average droplet sizes by over 70%, while keeping the basic jet structure and breakup mechanisms the same. This demonstrates that evaporation effects are not negligible and must be taken into account when performing injection studies.

This report shows that a new method proposed can be used to simulate a prototype case of fuel injection into a heated airstream with chilled fluid injection into an ambient temperature airstream. The process of jet breakup and vaporization can be visualized, and droplet measurements can be made under laboratory environment conditions. This method presents itself as an attractive alternative to complicated and expensive hot-flow testing.

Acknowledgment

This work was supported by the U. S. Air Force Office of Scientific Research, with Dr. J. Tischkoff as Technical Monitor.

References

[1] Williams, A., *Combustion of Sprays of Liquid Fuels*, The Gresham Press, Old Woking, England, 1976.

[2] Kush, E. and Schetz, J. A., "Liquid Injection into a Supersonic Flow," *AIAA Journal*, Vol. 11, Sept. 1973.

[3] Joshi, P. and Schetz, J. A., "Effect of Injector Shape on Penetration and Spread of Liquid Jets," *AIAA Journal*, Vol. 13, Sept. 1975, pp. 1137-1138.

[4] Baranovsky, S. I. and Schetz, J. A., "Effect of Injection Angle on Liquid Injection in Supersonic Flow," *AIAA Journal*, Vol. 18, June 1980, pp. 625-629.

[5] Schetz, J. A., McVey, W., and Padhye, R., "Studies of Transverse Liquid Fuel Jets in High-Speed Airstreams," Virginia Polytechnic Institute, Blacksburg, Rept. VPI-Aero-0.49.

[6] Sherman, A. and Schetz, J. A., "Break-up of Liquid Sheets and Jets in a Supersonic Gas Stream," *AIAA Journal*, Vol. 9, April 1971, pp. 666-673.

[7] Forde, J., Molder, S., and Szpiro, J., "Secondary Liquid Injection into a Supersonic Airstream," *Journal of Spacecraft and Rockets*, Vol. 3, Aug. 1966, pp. 1173-1176.

[8] Kolpin, M. A., Horn, K. P., and Reichenbach, R. E., "Study of a Liquid Injectant into a Supersonic Flow," *AIAA Journal*, Vol. 6, May 1968, pp. 853-858.

[9] Schetz, J. A. and Padhye, A., "Penetration and Break-up of Liquids in Subsonic Airstreams," *AIAA Journal*, Vol. 15, Oct. 1977, pp. 1385-1390.

[10] Reichenbach, R. E. and Horn, K. P., "Investigation of Injectant Properties on Jet Penetration in a Supersonic Stream," *AIAA Journal*, Vol. 9, March 1971, pp. 469-472.

[11] Nejad, A. S. and Schetz, J. A., "Effects of Properties and Location in the Plume on Mean Droplet Diameter for Injection in a Supersonic Stream," *AIAA Journal*, Vol. 21, No. 7, July 1983, pp. 956-961.

[12] Yule, A. J., "Sprays, Drops, Dusts, Particles," *Combustion and Flame*, Vol. 44, 1982, pp. 71-84.

[13] Simmons, H. C. and Harding, C. F., "Some Effects of Using Water as a Test Fluid in Fuel Nozzle Spray Analysis," ASME Paper 80-GT-90, Dec. 1979.

[14] Robers, J. H. and Webb, M. J., "Measurement of Droplet Size for Wide Range Particle Distribution," *AIAA Journal*, Vol. 2, March 1964, pp. 583-585.

[15] Gooderum, P. B. and Bushnell, D. M., "Atomization, Dropsize, and Penetration for Cross Stream Water Injection at High-Altitude Re-entry Conditions with Application to a RAM C-1 and C – III Flights," NASA-TND-6747, July 1972.

[16] Dobbins, R. A., Crocco, L., and Glassman, I., "Measurement of Mean Particle Sizes of Sprays from Diffractively Scattered Light," *AIAA Journal*, Vol. 1, Aug. 1963, pp. 1882-1886.

[17] Mugele, R. A. and Evans, H. D., "Droplet Size Distribution in Sprays," *Industrial and Engineering Chemistry*, Vol. 43, 1951, pp. 1317-1324.

[18] Situ, M. and Schetz, J. A., "Computational and Experimental Study of the Mass Transfer on Liquid Jet Break-up," AIAA Paper 83-1400, June 1983; also, *AIAA Journal* (to be published).